Energy and Buildings 152 (2017) 73–85

Contents lists available at ScienceDirect

Energy and Buildings

journal homepage: www.elsevier.com/locate/enbuild

PMV-based event-triggered mechanism for building energy management under uncertainties☆

Zhanbo Xu[a,*], Guoqiang Hu[b], Costas J. Spanos[c], Stefano Schiavon[d]

[a] Berkeley Education Alliance for Research in Singapore, 068898, Singapore
[b] School of Electrical and Electronic Engineering, Nanyang Technological University, 639798, Singapore
[c] Department of Electrical Engineering and Computer Sciences, University of California, Berkeley, CA 94720 USA
[d] Center for the Built Environment, Department of Architecture, University of California, Berkeley, CA 94720 USA

ARTICLE INFO

Article history:
Received 6 March 2017
Received in revised form 8 June 2017
Accepted 5 July 2017
Available online 14 July 2017

Keywords:
Building energy management
Event-triggered mechanism
Operational optimization
Predicted mean vote (PMV) index
Uncertainties in building operation

ABSTRACT

This paper provides a study of the optimal scheduling of building operation to minimize its energy cost under building operation uncertainties. Opposed to the usual way that describes thermal comfort using a static range of air temperature, the optimization of a tradeoff between energy cost and thermal comfort predicted mean vote (PMV) index is addressed in this paper. In order to integrate the calculation of the PMV index with the optimization procedure, we develop a sufficiently accurate approximation of the original PMV model which is computationally efficient. We develop a model-based periodic event-triggered mechanism (ETM) to handle the uncertainties in the building operation. Upon the triggering of predefined events, the ETM determines whether the optimal strategy should be recalculated. In this way, the communication and computational resources required can be significantly reduced. Numerical results show that the ETM method is robust with respect to the uncertainties in prediction errors and results in a reduction of more than 60% in computation without perceivable degradation in system performance as compared to a typical closed-loop model predictive control.

1. Introduction

Energy consumption worldwide is continuously increasing with the rise in living standards and the global population. Improving energy efficiency for end-users is an effective way to alleviate the energy crisis [1,2]. Building sector accounts for 40% of all primary energy consumption and more than 70% of electricity consumption [3]. One salient feature of the building operation is that its demand profiles are flexible due to the building thermal storage process and the elastic requirements of occupants. This flexibility provides a huge potential for building energy efficiency. Therefore, the optimization of building operation is becoming a necessity which has attracted more attention in recent years. With the sustaining development of smart microgrid technologies, many efforts have been made to optimize the building operation while satisfying the requirements of occupants. A basic optimization method is to develop building models that capture the system dynamics and requirements of occupants, and proceed to find the optimal solution based on these models.

Generally, there are three ways to develop a building performance/energy model that incorporates mechanical systems (heating, ventilation, and air conditioning – HVAC). First, one can develop a physics-based model using simulation software such as EnergyPlus [4] and TRNSYS [5]. A precise model is obtained this way, but it is time consuming and expensive to develop and requires immense computational resources. Second, the model can be developed using machine learning methods such as artificial neural networks [6] and regression models [7]. Although developing the model in this way is relatively easy and requires less computational resources, a lot of training data is required to produce a model with high prediction accuracies. Third, the model can be developed using simplified physics principles-based state equations of building thermal dynamics such as the models developed in [8–10]. This type of the models is simpler than simulation-based models, but it can address tradeoffs between accuracy and com-

☆ This work was supported by the Republic of Singapore's National Research Foundation through a grant to the Berkeley Education Alliance for Research in Singapore (BEARS) for the Singapore-Berkeley Building Efficiency and Sustainability in the Tropics (SinBerBEST) Program. BEARS has been established by the University of California, Berkeley as a center for intellectual excellence in research and education in Singapore.

* Corresponding author.
E-mail addresses: zhanbo.xu@bears-berkeley.sg (Z. Xu), gqhu@ntu.edu.sg (G. Hu), spanos@berkeley.edu (C.J. Spanos), stefanoschiavon@berkeley.edu (S. Schiavon).

http://dx.doi.org/10.1016/j.enbuild.2017.07.008
0378-7788/

putational resources. In general, the last two types of the modeling methods are usually used for various optimization and control purposes. For example, based on the second type of the methods, an optimization problem was developed in [6] to capture a tradeoff between energy saving and thermal comfort level, a multi-objective optimization of energy consumption and thermal comfort was formulated in [7], and optimal control problems for HVAC system were developed in [10,24] respectively. Based on the third type of the methods, an optimization problem of a tradeoff between energy saving and air quality was developed in [8], an optimal scheduling problem for energy devices in smart homes was formulated in [9], and an joint control problem of active and passive heating, cooling, lighting, shading, and ventilation in buildings was addressed in [25].

Based on the models mentioned above, many optimization methods have been developed to facilitate building energy efficiency. For example, mixed integer programming is such a conventional method, since the problem always contains both continuous and discrete variables [9,11]. Model predictive control (MPC) is another method usually used to address the problem under uncertainties. Existing results obtained in [10,12,13] showed that MPC features high energy and cost saving since the future evolution of system dynamics is involved in the decision-making process and the optimal solution is obtained based on a rolling horizon basis. Kwadzogah et al. [13] provided a review of MPC for HVAC systems. Event-based optimization methods have recently been applied to building energy efficiency such as in [14,15]. This type of the methods is computationally efficient for solving large-scale problems since their state space can be significantly reduced by the events defined by a set of state transitions. In addition, many other methods, such as genetic algorithms [7,18], fuzzy control [16,17], simulation-based optimization methods [4,5], etc., were attempted. The above literature showed that 10%–30% of energy consumption (costs) can be reduced by the optimization of building operation.

However, building operational optimization still faces many challenges, two of which that are very relevant are a high level of thermal discomfort and uncertainties in building operations. Regardless of the high energy consumption, a majority of occupants are still not satisfied with their thermal environment [19]. Therefore, an elaborate model for describing occupants' thermal comfort should be involved in the optimization of the building operation. Since the thermal comfort of occupants is mainly determined by the indoor air temperature, mean radiant temperature, humidity, air velocity, metabolic activity and clothing insulation, the selected model needs to reflect the influence of the above factors on thermal comfort, such as in the well-known predicted mean vote (PMV) model [20]. However, it may be computationally expensive to directly integrate the PMV model with the optimization procedure due to its non-convex and nonlinear properties. Building demand profiles feature impactful uncertainties due to random weather conditions and occupants behaviors. Both of these uncertainties have a significant impact on the building energy efficiency and thus need to be addressed. Many methods have been proposed to handle these uncertainties, but most of them, such as MPC and rolling horizon methods, are time-triggered. Through the time-triggered methods, the optimal solution is recalculated once at each sampling stage. However, the recalculation at stages when the building system is operating within a desirable range is clearly a waste of communication and computational resources, which may make the broad deployment of such methods unnecessarily costly, especially for large-scale building systems.

A typical control system for the building operation includes two levels. The goal of the upper level is to obtain an optimal scheduling strategy of the energy devices to minimize energy cost or consumption while satisfying the thermal requirements of occupants. The goal of the lower level is to adjust the local actuators to track the scheduling strategy obtained from the upper level. In this paper, we focus on the scheduling problem of the building operation in the upper level. Through addressing the challenges mentioned before, we make the following contributions. First, an optimal scheduling problem of the building operation is developed based on a steady state model for building energy dynamics to capture a tradeoff between the energy cost and the PMV index. In this problem, we develop a piecewise linearization-based approximation of the original PMV model to predict the thermal comfort of occupants. This approximate PMV model does not introduce significant errors but is computationally efficient for the optimization purpose. It is also found that compared to the usual way that describes the thermal comfort by a static range of indoor air temperature, the proposed model provides more flexibility and hence exhibits more potential on both energy cost savings and demand reduction. Second, we develop a model-based periodic event-triggered mechanism (ETM) to handle the uncertainties in the building operation especially those in the outdoor temperature, solar radiation, usage pattern of electrical appliances, and occupancy. Upon triggering of two events defined by the state transitions of the occupancy and thermal comfort of occupants, the ETM determines whether the optimal strategy should be recalculated at each stage. In this way, the communication and computational resources can be significantly reduced. Third, the performance of the ETM method is tested based on an office-room environment in Singapore. Numerical results show that the ETM method is robust with respect to uncertainties in prediction error, and it can reduce the communication and computational resources by more than 60% without perceivable degradation in the system performance as compared to a typical closed-loop MPC method.

The rest of the paper is organized as follows. The problem formulation is presented in Section 2. The approximate PMV model and the ETM method are developed in Section 3. In Section 4, the performances of the approximate PMV model and the ETM method are evaluated and validated using case studies of an experiment in Singapore. The discussion for the proposed work and the conclusions are given in Sections 5 and 6 respectively.

2. Problem formulation

A daily scheduling problem of the building operation based on a discrete-time formulation is presented in this section. The scheduling horizon, i.e., 24 h, is discretized into K stages. The objective is to minimize the building electricity cost in response to a time-of-use (TOU) electricity price over the scheduling horizon, while satisfying the thermal comfort of occupants. This problem formulation is developed based on an office-room environment in Singapore. In the following, the models for the thermal comfort of occupants and the room energy dynamics are presented in Sections 2.1 and 2.2 respectively. The objective function is shown in Section 2.3.

2.1. Model for thermal comfort of occupants

In most of the existing studies on the optimization of building operation, the thermal comfort of occupants is usually described by a static range of indoor air temperature, since it would not provide any computational challenges to solving the optimization problem. However, describing the thermal comfort by a static range of indoor air temperature is conservative and inadequate since it is determined by six main variables of environmental factors (which are the indoor air temperature, mean radiant temperature, relative humidity, and air velocity) and personal factors (which are the clothing and metabolic rate of the occupant). We select the well-known PMV model in this paper to elaborately describe the thermal comfort of

occupants. It establishes a mapping from the six main factors to the thermal comfort index scale of [−3, +3], which is given by [20]:

$$PMV = [0.303 \cdot \exp(-0.036 \cdot M) + 0.028] \cdot L, \quad (1)$$

normalsize

$$L = (M - W) - 3.05 \times 10^{-3} \cdot [5733 - 6.99 \cdot (M - W) - P_a] - 0.42 \cdot [(M - W) - 58.15] - 1.7 \times 10^{-5} \cdot M \cdot (5867 - P_a) - 0.0014 \cdot M \cdot (34 - t_a) - 3.96 \times 10^{-8} \cdot f_{cl} \cdot [(t_{cl} + 273)^4 - (\overline{t_r} + 273)^4] - f_{cl} \cdot h_c \cdot (t_{cl} - t_a), \quad (2)$$

normalsize

$$t_{cl} = 35.7 - 0.028 \cdot (M - W) - I_{cl}\{3.96 \times 10^{-8} \cdot f_{cl} \cdot [(t_{cl} + 273)^4 - (\overline{t_r} + 273)^4] + f_{cl} \cdot h_c \cdot (t_{cl} - t_a)\}, \quad (3)$$

$$h_c = \begin{cases} 2.38 \cdot |t_{cl} - t_a|^{0.25} \; if 2.38 \cdot |t_{cl} - t_a|^{0.25} > 12.1\sqrt{v_{ar}}, \\ 12.1\sqrt{v_{ar}} \quad if 2.38 \cdot |t_{cl} - t_a|^{0.25} \le 12.1\sqrt{v_{ar}}, \end{cases} \quad (4)$$

$$f_{cl} = \begin{cases} 1 + 1.29 \cdot I_{cl} \quad if I_{cl} \le 0.078, \\ 1.05 + 0.645 \cdot I_{cl} \;\; if I_{cl} > 0.078, \end{cases} \quad (5)$$

$$P_a = h_r \cdot 6.1094 \cdot \exp[(17.625 \cdot t_a)/(t_a + 243.04)], \quad (6)$$

where PMV is the value of the PMV index, M is the metabolic rate (in W/m^2), L is the thermal load of human body (in W/m^2), W is the rate of mechanical work (in W/m^2), P_a is the water vapor pressure (in Pa), t_a is the indoor air temperature (in °C), t_{cl} is the clothing surface temperature (in °C), $t_{\overline{r}}$ is the mean radiant temperature (in °C), f_{cl} is the clothing surface area factor, I_{cl} is the clothing insulation (in m^2 K/W), h_c is the convective heat transfer coefficient (in W/(m^2 K)), v_{ar} is the air velocity (in m/s), and h_r is the relative humidity (in%). In (1)–(6), the superscript k (k = 0,1,. . .,K-1) indicating the stage index is omitted for simplification. The values of indoor air temperature and relative humidity can be directly measured with the corresponding sensors. The values of the metabolic rate and clothing insulation can be estimated by prior knowledge, referring to standards such as in [22,23]. In most of the office buildings, cooling fans are not present, so the indoor air velocity in a mechanically ventilated office environment is low and usually less than 0.2 m/s [21,23]. Air velocity is not measured due to the cost of the sensors and we assumed that it is equal to 0.18 m/s in the case studies in this paper. The clothing surface temperature, convective heat transfer coefficient, clothing surface area factor, and water vapor pressure can be calculated with the formulas in (3)–(6), respectively. The mean radiant temperature can be measured directly, estimated by the area-weighted mean temperature of the interior surface of all walls in the room [21], or deduced from the operative temperature if known. In this paper, we used the second method, although any of them can be utilized in our approach.

As mentioned earlier, the PMV model is elaborate for describing the thermal comfort of occupants. But it may provide a computational challenge to directly solving the optimization problem due to its non-convex and nonlinear properties. Therefore, in this paper, we develop a piecewise linearization-based approximation of the original PMV model for the optimization purpose, the details of which are shown in Section 3.1.

When the room is occupied, the PMV value which is calculated with the thermal environment should be limited to a given comfortable range. So the constraint for the thermal comfort of occupants at stage k is given by:

$$P_{\min} \cdot z_a^k - 3 \cdot (1 - z_a^k) \le PMV^k \le P_{\max} \cdot z_a^k + 3 \cdot (1 - z_a^k), \quad (7)$$

where $P_{\min}$ and $P_{\max}$ are the lower and upper bounds of the comfortable range respectively, which can be obtained by statistical sampling of actual data with the occupants' feedback or by thermal comfort standards, z_a^k is an integer variable where $z_a^k = 1$ means that the room is occupied at k, otherwise, $z_a^k = 0$.

2.2. Model for building energy dynamics

Since the main focus of this paper is to evaluate the performance of the proposed ETM method in the application of the building operational optimization, in this paper we use two generic models developed in [24,25] to formulate the room energy dynamics. The resistance-capacitance (RC) network-based model developed in [24] is used to describe the temperature dynamics of indoor air and wall surface. This model can be used for different weather conditions. For example, it was validated for winter in [24] and for summer in [33]. The HVAC model developed in [25] is used to formulate the energy consumption and thermal energy supplied by HVAC. Through this HVAC model, the control of indoor air temperature and humidity and natural ventilation can be involved. In order to use these models with high accuracy, the parameters in the two models need to be identified for a specific application. Therefore, we conducted an experiment in an office room in Singapore to identify and verify the two models mentioned above for the case studies in this paper. In other words, the room model developed in this paper is derived from the two generic models with the actual data. Moreover, we notice that any generic/specific room model can be deployed in the proposed ETM method and may have no impact on its performance, since the ETM method does not depend on the room model. The details for this discussion will be provided in Section 5.

Since the building considered in the experiment is pressurized and the corresponding room has a closed window, natural ventilation and infiltration are not involved in the room model. However, we notice that natural ventilation does not provide any particular complexity in the application of the proposed ETM method. The details of the model for natural ventilation can be found in [25]. In the room, the indoor air temperature (i.e., major part of the sensible load) is controlled by the fan coil unit (FCU) and the indoor humidity and air quality (i.e., latent load and other part of the sensible load caused by outdoor air) are controlled by a dedicated outdoor air system (DOAS). Therefore, the energy dynamics of the room can be developed as follows.

In the RC network-based model, indoor air and wall surface temperatures are considered as two types of nodes in the network. For each node, its temperature dynamics is formulated based on the heat exchange with all neighboring nodes. Assume that there are a total of W walls in the room. For the w-th (w = 1,2,. . .,W) wall, its temperature dynamics is given by [24]:

$$C_{ww}(t_{ww}^{k+1} - t_{ww}^k) = \tau \cdot \left[\sum_{j \in N_{ww}} (t_j^k - t_{ww}^k)/R_{ww,j} + \gamma_w \alpha_w A_w q_{ww}^k \right], \quad (8)$$

where C_{ww}, α_w, and A_w are the heat capacity (in J/K), absorption coefficient, and area (in m^2) of the wall w respectively, t_{ww}^k is the surface temperature of the wall w at k (in °C), τ is the length of time in each stage (in s), N_{ww} is the set of neighboring nodes to the wall w node, t_j^k is the temperature of the j-th neighboring node at k (in °C), $R_{ww,j}$ is the thermal resistance between wall w and its j-th neighboring node (in K/W), γ_w is equal to 0 for internal walls and 1 for external walls, and q_{ww}^k is the solar radiation density on wall w at k (in W/m^2). The first term on the right-hand-side (RHS) of (8) indicates the heat exchange with all neighboring nodes and the second term indicates the thermal gain from solar radiation for external walls.

The temperature dynamics of the indoor air is given by [24]:

$$C_a(t_a^{k+1} - t_a^k) = \tau \cdot \left[\sum_{j \in N_a} (t_j^k - t_a^k)/R_{a,j} + G_{fcu}^k c_p (t_{fcu}^k - t_a^k) + G_{doas}^k c_p (t_{doas}^k - t_a^k) + \beta_{win} A_{win} q_{sa}^k + q_{in}^k \right], \quad (9)$$

where C_a is the heat capacity of the indoor air (in J/K), t_a^k is the indoor air temperature at k (in °C), N_a is the set of neighboring nodes to the node of indoor air, $R_{a,j}$ is the thermal resistance between the node of indoor air and its j-th neighboring node (in K/W), G_{fcu}^k and t_{fcu}^k are the outlet mass flow rate (in kg/s) and outlet temperature (in °C) of the FCU at k respectively, c_p is the specific heat of the air (in J/kg°C), G_{doas}^k and t_{doas}^k are the mass flow rate (in kg/s) and temperature (in °C) of the air supplied by the DOAS at k respectively, β_{win} is the transmissivity of the window glass, A_{win} is the area of the window (in m^2), q_{sa}^k is the solar radiation density radiated into the room from the window at k (in W/m^2), and q_{in}^k is the internal heat generation at k (in W), such as heat gain from occupants, electrical appliances, and furniture. The RHS of (9) formulates the heat exchange with all neighboring nodes, the cooling supplied by the FCU and DOAS, the external heat gain through the window, and the internal heat gain respectively. The parameters in (8)–(9), such as the values of the capacitance and resistance for each node, can be identified with the measured data of the indoor air temperature, wall surface temperature, and external and internal heat gains. The accuracy of this room model is validated in Section 4.2.

The indoor humidity controlled by the DOAS is given by [25]:

$$m_a(h_a^{k+1} - h_a^k) = \tau \cdot [O^k h_g + G_{doas}^k (h_{doas}^k - h_a^k)], \quad (10)$$

where m_a is the mass of the indoor air (in kg), h_a^k is the indoor humidity ratio at k (in kg/kg), O^k is the number of occupants in the room at k, h_g is the humidity generation ratio per person (in kg/s), and h_{doas}^k is the set-point of air humidity ratio provided by the DOAS at k (in kg/kg). Eq. (10) shows that the indoor humidity dynamics is determined by the humidity generated by occupants, the effect of DOAS, and the resultant humidity content in the indoor air [25]. The effect of furnishing and building materials on the humidity level in the space is not considered.

The desired indoor thermal environment is provided and maintained by the HVAC system, and it is also affected by the heat generation of electrical appliances such as lighting, computers, and monitors. The models of these appliances are shown in the following.

The cooling supplied by the FCU and DOAS is equal to the enthalpy between their inlet and outlet airs [25], so we have:

$$q_{fcu}^k = \{\tau \cdot G_{fcu}^k [c_p t_a^k + h_a^k (2500 + 1.84 t_a^k)] - \tau \cdot G_{fcu}^k [c_p t_{fcu}^k + h_a^k (2500 + 1.84 t_{fcu}^k)]\}/(3.6 \times 10^6), \quad (11)$$

$$q_{doas}^k = \{\tau \cdot G_{doas}^k [c_p t_o^k + h_o^k (2500 + 1.84 t_o^k)] - \tau \cdot G_{doas}^k [c_p t_{doas}^k + h_{doas}^k (2500 + 1.84 t_{doas}^k)]\}/(3.6 \times 10^6), \quad (12)$$

where q_{fcu}^k and q_{doas}^k are the cooling energy supplied (in kWh) by the FCU and DOAS at k respectively, and t_o^k and h_o^k are the outdoor temperature (in °C) and humidity ratio (in kg/kg) at k respectively.

The electricity consumption of the fans in the FCU and DOAS can be formulated in the same way. In this paper, we use the FCU as an example to show this energy consumption model. The outlet mass flow rate of the FCU is typically set at various discrete levels. Without loss of generality, assume that there are a total of V discrete levels of the outlet mass flow rate, where g_v indicates the v-th discrete value. Based on the model developed in [25], the electricity consumption of the fan in the FCU is given by:

$$\begin{cases} e_{fcu}^k = p_{rated} \cdot \tau \cdot \sum_{v=1}^{V} x_v^k \cdot (g_v / G_{rated})^3 / 3600, \\ G_{fcu}^k = \sum_{v=1}^{V} x_v^k \cdot g_v, \ \sum_{v=1}^{V} x_v^k \le 1, \end{cases} \quad (13)$$

where e_{fcu}^k is the electricity consumption of the fan in the FCU at k (in kWh), p_{rated} and G_{rated} are the rated power (in kW) and rated outlet mass flow rate (in kg/s) of the FCU respectively, and x_v^k is an integer variable. $x_v^k = 1$ means that the outlet mass flow rate equals to g_v (in kg/s) at k; otherwise, $x_v^k = 0$. For the fan in the DOAS, its electricity consumption, e_{doas}^k (in kWh), can be formulated in the same way as in (13) with the corresponding variables and parameters.

Since this paper focuses on the thermal comfort of indoor environment, the electricity consumption of other parts of the HVAC is estimated by the coefficient of performance (COP) of the chiller. It is thus given by:

$$e_{hvac}^k \cdot cop^k = q_{fcu}^k + q_{doas}^k \le q_{hvac}, \quad (14)$$

where e_{hvac}^k is the electricity consumption of the chiller in the HVAC at k (in kWh), cop^k is the COP of the chiller at k, and q_{hvac} is the cooling capacity of the HVAC (in kWh). The COP of the chiller is determined by the cooling load of the HVAC, which can be obtained by fitting the actual data of electricity consumption and cooling supplied by the HVAC. In this paper, a mapping from the electricity consumption to the cooling supplied is developed based on the measured data in different conditions of the cooling load, which is then piecewise linearized with high accuracy. The mapping and its piecewise linearization are shown in Section 4.2.

The electricity consumption of the lighting is determined by the indoor illuminance demand and occupancy. The constraint of the lighting operation is thus given by:

$$\begin{cases} I_d^k + e_{light}^k \cdot I_{light} \ge I_{load} \cdot z_a^k, \\ Q_{light}^k = e_{light}^k \cdot \mu_l, \end{cases} \quad (15)$$

where I_d^k is the illuminance supplied by the daylight at k (in lx), e_{light}^k is the electricity consumption of the lighting at k (in kWh), I_{light} is the illuminance supplied by the lighting per kWh (in lx/kWh), I_{load} is the indoor illuminance demand (in lx), Q_{light}^k is the heat generation of the lighting at k (in kWh), and μ_l is the coefficient of heat generation per kWh of the lighting.

Computers and monitors are the most common electrical appliances in an office-room environment. In this paper, their electrical power usage is assumed to be constant during their operation. Since their operation is determined by the presence of occupants, their electricity consumption (in kWh), e_c^k, and heat generation (in kWh), Q_c^k, are given by:

$$e_c^k = p_c \cdot \tau \cdot O^k / 3600, \ Q_c^k = \mu_c \cdot e_c^k, \quad (16)$$

where p_c is the mean power of the summation of that of the computers and monitors (in kW), and μ_c is the coefficient of their heat production per kWh.

The simplifications on the modeling of the heat and mass transfer of the problem introduced in this section are needed for the proper use of optimization [25].

2.3. Objective function

The objective of the scheduling problem is to determine the operation of energy devices in response to a specific electricity price signal such that the overall electricity cost is minimized over the scheduling horizon, while satisfying the thermal requirements of occupants. The objective function is given by:

$$\min \sum_{k=0}^{K-1} c^k \cdot (e^k_{hvac} + e^k_{fcu} + e^k_{doas} + e^k_{light} + e^k_c), \tag{17}$$

where c^k is the electricity price at k (in S$/kWh). The objective function should be subject to the constraints consisting of (1)–(16). The optimization problem consisting of (1)–(17) is a mixed integer nonlinear programming problem due to the presence of the PMV model. In the next section, a piecewise linearization-based approximation of the original PMV model is presented. Based on this approximate PMV model, the problem can be reformulated as a mixed integer linear programming problem which can be efficiently solved.

3. Solution methodology

As mentioned before, it may be computationally expensive or even infeasible to solve the optimization problem involving the PMV model. To overcome this challenge, an approximate PMV model is developed in Section 3.1, which is sufficiently accurate and computationally efficient for the optimization purpose. Furthermore, in order to efficiently handle the uncertainties in the building operation, a model-based periodic ETM method is developed in Section 3.2.

3.1. Piecewise linearization of the original PMV model

As shown in (1)–(6), the PMV model is non-convex and nonlinear due to the presence of the nonlinearities in (2)–(4) and (6). In (2) and (3), there are the same nonlinearities caused by the nonlinear functions of the clothing surface temperature and the mean radiant temperature, Eq. (4) is nonlinear due to the presence of the "if-else" conditions, and (6) is nonlinear due to the product of the relative humidity and the exponential function of the air temperature.

In this paper, we use piecewise linearization to approximate the original PMV model, i.e., the nonlinearities in (2), (3), and (6) are piecewise linearized with respect to the ranges of the indoor air temperature, the mean radiant temperature, and the clothing surface temperature. The usual ranges of these variables are divided into F, L, and I segments respectively. Within each segment, the nonlinearities are approximated by linear functions. For each segment, the slopes and intercepts of the linear functions can be calculated by the original PMV model with the values of two endpoints in this segment. Through introducing integer variables for each segment, the nonlinearities in (2), (3), and (6) are linearized as follows:

$$(t_{cl}+273)^4 - (\overline{t_r}+273)^4 = \sum_{i=1}^{I}(a_{cl,i}\cdot t_{cl,i} + b_{cl,i}\cdot z_{cl,i}) - \sum_{l=1}^{L}(a_{tr,l}\cdot t_{tr,l} + b_{tr,l}\cdot z_{tr,l}), \tag{18}$$

$$P_a = \sum_{f=1}^{F} h_r(a_{ta,f}\cdot t_{a,f} + b_{ta,f}\cdot z_{ta,f}), \tag{19}$$

$$\begin{cases} \sum_{i=1}^{I} z_{cl,i} = 1,\ t_{cl} = \sum_{i=1}^{I} t_{cl,i}, \\ z_{cl,i}\cdot t^{\min}_{cl,i} \le t_{cl,i} \le z_{cl,i}\cdot t^{\max}_{cl,i}, \end{cases} \tag{20}$$

$$\begin{cases} \sum_{l=1}^{L} z_{tr,l} = 1,\ \overline{t_r} = \sum_{l=1}^{L} t_{tr,l}, \\ z_{tr,l}\cdot t^{\min}_{tr,l} \le t_{tr,l} \le z_{tr,l}\cdot t^{\max}_{tr,l}, \end{cases} \tag{21}$$

$$\begin{cases} \sum_{f=1}^{F} z_{ta,f} = 1,\ t_a = \sum_{f=1}^{F} t_{a,f}, \\ z_{ta,f}\cdot t^{\min}_{ta,f} \le t_{a,f} \le z_{ta,f}\cdot t^{\max}_{ta,f}, \end{cases} \tag{22}$$

where $t_{cl,i}$, $t_{tr,l}$, and $t_{a,f}$ are the values of the clothing surface temperature in the i-th segment of its range, the mean radiant temperature in the l-th segment of its range, and the indoor air temperature in the f-th segment of its range respectively, $a_{cl,i}$, $b_{cl,i}$, $a_{tr,l}$, $b_{tr,l}$, $a_{ta,f}$, and $b_{ta,f}$ are the slopes and intercepts of the linear functions in the corresponding segments for approximating the nonlinearities respectively, $z_{cl,i}$, $z_{tr,l}$, and $z_{ta,f}$ are integer variables for the clothing surface temperature, the mean radiant temperature, and the indoor air temperature in the corresponding segments respectively. These integer variables are defined in the same way. For instance, $z_{cl,i} = 1$ means that the clothing surface temperature is within its i-th segment, and otherwise, $z_{cl,i} = 0$. $t^{\min}_{cl,i}$, $t^{\max}_{cl,i}$, $t^{\min}_{tr,l}$, $t^{\max}_{tr,l}$, $t^{\min}_{ta,f}$, and $t^{\max}_{ta,f}$ are the lower and upper bounds of the clothing surface temperature, the mean radiant temperature and the indoor air temperature in the corresponding segments respectively. By (18), (20), and (21), the nonlinearities in (2) and (3) are piecewise linearized. However, in (19), the calculation of water vapor pressure is still nonlinear due to the product of the relative humidity and the piecewise linear function of the indoor air temperature.

We use the following method to achieve the linearization of (6) by (19) and (22). Through the ETM method shown in Section 3.2, the operational strategy should be recalculated when the predefined events are triggered. For each recalculation of the optimal strategy, the relative humidity over all stages is calculated based on currently measured data with the optimal trajectory calculated from the last time step in advance, i.e., the relative humidity is regarded as a parameter in the new recalculation of the operational strategy. In this way, the water vapor pressure in (19) is a piecewise linear function of the indoor air temperature that is constrained by (22). This approximation of the relative humidity is reasonable since the impact of the variance in the relative humidity on thermal comfort is small at moderate temperatures close to comfort and may usually be disregarded when determining the PMV value [23]. In addition, the mismatch caused by this approximation can be compensated by the triggering of the events and moving horizon scheme used in the ETM method. Therefore, based on the above approximation, the nonlinearities in (2), (3), and (6) can be piecewise linearized by (18)–(22).

Since the difference between the indoor air temperature and the clothing surface temperature is generally small in practice [21,22], the convective heat transfer coefficient is always calculated by the second equation of (4). Therefore, the second equation of (4) is used instead of the "if-else" conditions in (4). In this way, the convective heat transfer coefficient can be calculated with the air velocity in advance and thus be regarded as a parameter in the model.

By calculating the relative humidity and the convective heat transfer coefficient in the above ways and replacing the nonlinearities in the PMV model by (18)–(22), the PMV value can be computed by a piecewise linear model consisting of (1)–(3), (5), and (18)–(22). The accuracy of this approximate PMV model is validated in Section 4.1. Using the above approximate PMV model, the scheduling prob-

lem developed in this paper is a mixed integer linear programming problem, and it can be reformulated as:

$$\min \sum_{k=0}^{K-1} c^k \cdot (e^k_{hvac} + e^k_{fcu} + e^k_{doas} + e^k_{light} + e^k_c), \tag{23a}$$

$$\text{s.t.} \mathbf{x}^{k+1} = \mathbf{A}\mathbf{x}^k + \mathbf{B}\mathbf{u}^k + \mathbf{E}\mathbf{d}^k, \tag{23b}$$

$$y^k = \mathbf{C}\mathbf{x}^k, \tag{23c}$$

$$\underline{U} \le \mathbf{u}^k \le \bar{U}, \underline{X} \le \mathbf{x}^k \le \bar{X}, \tag{23d}$$

$$P_{\min} \cdot z^k_a - 3 \cdot (1 - z^k_a) \le y^k \le P_{\max} \cdot z^k_a + 3 \cdot (1 - z^k_a), \tag{23e}$$

where $\mathbf{x}^k$ is the state vector at k, which is denoted by: $\mathbf{x}^k = [t^k_a, h^k_a, \bar{t}^k_r, t^k_{cl}, h^k_r, p^k_a, t^k_{ww}], \forall w = 1, 2, \ldots, W$, $\mathbf{u}^k$ is the input vector at k, which includes two parts: the intermediate variables of the problem at k, i.e., $[G^k_{fcu}, G^k_{doas}, q^k_{fcu}, q^k_{doas}, e^k_{fcu}, e^k_{doas}, e^k_{hvac}, Q^k_{light}, e^k_c, Q^k_c]$, and the decision variables of the problem at k, i.e., $[t^k_{fcu}, h^k_{doas}, x^k_v, e^k_{light}, t^k_{cl,i}, z^k_{cl,i}, t^k_{tr,l}, z^k_{tr,l}, t^k_{a,f}, z^k_{ta,f}], \forall v = 1, 2, \ldots, V, i = 1, 2, \ldots, I, l = 1, 2, \ldots, L, f = 1, 2, \ldots, F$, $\mathbf{d}^k$ is the disturbance vector at k, which is denoted by: $\mathbf{d}^k = [z^k_a, q^k_{ww}, q^k_{sa}, q^k_{in}, O^k, t^k_o, h^k_o], \forall w = 1, 2, \ldots, W$, y^k is the output scalar at k representing the PMV value, and **A**, **B**, **C**, and **E** are the matrices of proper dimensions which can be obtained from (1)–(22) respectively. Eq. (23a) is the objective function, which is equivalent to (17). Eq. (23b) describes the indoor thermal dynamics corresponding to (8)–(10). Eq. (23c) represents the calculation of the PMV index corresponding to (1)–(3), (5), and (18)–(19). Eq. (23d) describes the constraints of the input and state variables, which corresponds to (11)–(16) and (20)–(22). Eq. (23e) is equivalent to (7), which represents the thermal requirements of occupants at each stage.

3.2. Event-triggered mechanism

Uncertainties are associated with many processes of the building operation. Among them, we consider the uncertainties in the outdoor temperature, solar radiation, occupied time of room, number of occupants, and usage pattern of electrical appliances in this paper, since they have a significant impact on the building demand profiles and thermal comfort. In this paper, a model-based periodic ETM method which is shown in Fig. 1 is developed to handle the uncertainties mentioned above in the optimization of the building operation. Note that based on (16), the uncertainty in the usage pattern of computers and monitors is determined by the room occupancy, so this uncertainty is combined into the uncertainty in the number of occupants.

The uncertainties can be considered to be the difference between the actual and predicted values of the disturbance in (23b), i.e.,

$$\mathbf{d}^k = \hat{\boldsymbol{d}}^k + \boldsymbol{w}^k, \|\mathbf{w}^k\|_\infty \le \lambda, k = 0, 1, \ldots, K-1, \tag{24}$$

where $\hat{\boldsymbol{d}}^k$ is the disturbance prediction vector at k representing the predicted values of the disturbance in (23b), and $\mathbf{w}^k$ is the stochastic disturbance vector at k, which is assumed to be bounded by λ as in [10]. Note that for any vector $\mathbf{s} = (s_1, s_2, \ldots, s_n)$, $\|\mathbf{s}\|_\infty := \max(|s_1|, |s_2|, \ldots, |s_n|)$.

The main idea of the model-based periodic ETM method is to determine whether the optimal strategy should be recalculated upon the triggering of the predefined events on a moving horizon scheme. At any stage, if any predefined event is triggered, the scheduling problem should be recalculated with the future evolution of the system dynamics to obtain the optimal solution. This future evolution is obtained by the system model with the current system state and predictions of the disturbance. On the contrary, if no event is triggered, the latest strategy is still executed. In this way, the communication and computational resources may be reduced. The details of the model-based periodic ETM method can be referred to [26].

The key to handle the uncertainties by the ETM method is in defining the proper events that can capture a tradeoff between the system performance and computational efficiency. Since the occupancy and thermal comfort of occupants are strongly related to the performance of the problem considered in this paper, we define the following two events based on the state transitions [27,28] to handle the uncertainties in the disturbance shown in (23b).

Event 1 is linked to occupancy which captures the uncertainty in the occupied time. As shown in (23e), the occupied time determines the lower and upper bounds of the thermal requirements. Hence, the triggering of event 1 caused by the uncertainty in the occupied time guarantees the exact identification of the thermal requirements in the room. We define that event 1 is triggered if the actual value of the occupied time is different from its predicted value. In this paper, when the optimal strategy should be recalculated at any stage k, all predicted values of the occupied time from stages $k+1$ to $k+N$-1 are generated with historical data, where N is the prediction horizon. In this way, event 1 may not frequently be triggered since the occupied time is always regular, especially in the office environment.

Since the thermal comfort of occupants, which constrains the system dynamics, may be changed by the variance of the disturbance, event 2 is defined by the state transition of the PMV value when the room is occupied. As shown in (23b)–(23c), event 2 captures the uncertainties in the disturbance vector outside the

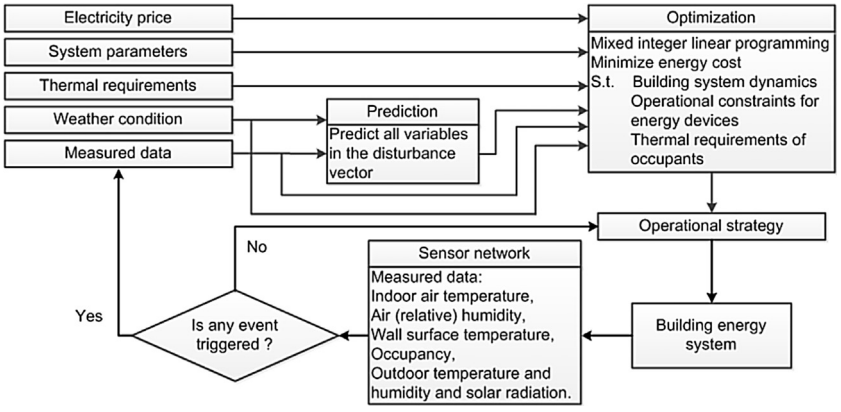

Fig. 1. The framework of the proposed event-triggered mechanism.

occupied time. To define event 2, the range of the PMV index is divided into three intervals: $[-3, P_{\min})$, $[P_{\min}, P_{\max}]$, and $(P_{\max}, +3]$. In order to satisfy the thermal requirements of occupants, event 2 is triggered when the PMV value deviates from the comfortable interval, i.e., $[P_{\min}, P_{\max}]$. Therefore, the triggering of event 2 guarantees the satisfaction of the thermal comfort of occupants over the scheduling horizon.

Based on these two predefined events, an ETM-based algorithm is developed to solve the optimization problem under the uncertainties in the disturbance.

Algorithm:

Step 1: Set $k = 0$. At stage 0, obtain the initial operational strategy by solving the problem in (23) with currently measured data and predictions of the disturbance over the scheduling horizon.

Step 2: Set $k = k + 1$. Based on the measured data at stage k and the current strategy, check if either event 1 or event 2 is triggered. If no event was triggered, apply the current strategy and go to step 4; otherwise, go to step 3.

Step 3: Update the predictions of all variables in the disturbance vector over N future stages with currently measured data. Then update the strategy by solving the following problem:

$$
\begin{aligned}
&\min \sum_{n=k}^{k+N-1} c^{(n|k)}\left(e_{hvac}^{(n|k)} + e_{fcu}^{(n|k)} + e_{doas}^{(n|k)} + e_{light}^{(n|k)} + e_{c}^{(n|k)}\right)\\
&\text{s.t.}\mathbf{x}^{(n+1|k)} = \mathbf{A}\mathbf{x}^{(n|k)} + \mathbf{B}\mathbf{u}^{(n|k)} + \mathbf{E}\mathbf{d}^{(n|k)},\\
&y^{(n|k)} = \mathbf{C}\mathbf{x}^{(n|k)},\\
&\underline{U} \le \mathbf{u}^{(n|k)} \le \bar{U}, \underline{X} \le \mathbf{x}^{(n|k)} \le \bar{X},\\
&y^{(n|k)} \ge P_{\min} \cdot z_a^{(n|k)} - 3 \cdot (1 - z_a^{(n|k)}),\\
&y^{(n|k)} \le P_{\max} \cdot z_a^{(n|k)} + 3 \cdot (1 - z_a^{(n|k)}),\\
&n = k, k+1, \ldots, k+N-1,\\
&\mathbf{x}^{(k|k)} = \mathbf{x}^{k}, \mathbf{x}^{(k+N|k)} \in X_{fs},
\end{aligned}
\tag{25}
$$

where superscript $(n|k)$ indicates the corresponding variable for the stage n predicted at stage k, and X_{fs} indicates the constraint of the terminal state. Note that the current state, $\mathbf{x}^k$, can be obtained from sensor networks in the building.

Step 4: If $k = K$-1, go to step 5; otherwise, go to step 2.

Step 5: Stop.

Remarks:

1. Recall that to solve the problem in (25) at each stage when any event is triggered, we need to calculate the relative humidity based on the optimal trajectory calculated by the latest strategy with currently measured data. For the first calculation of the operational strategy at stage 0, the relative humidity over all stages can be generated with historical data or empirical knowledge.
2. As mentioned before, the problem in (25) is a mixed integer linear programming problem. Many computationally efficient methods have been developed to solve this type of problem, such as the CPLEX solver for the small or medium-scale problem and the methods developed in [14,15,29], for the large-scale problem.
3. The measured data at each stage consist of the indoor air temperature, (relative) air humidity, wall surface temperature, occupancy, solar radiation, outdoor temperature, and outdoor humidity, which can be collected by sensor networks in the building. We assume that the measured data are accurate, since the measurement error of the sensor networks is beyond of the scope of this paper.
4. In this paper, the occupancy state is detected by the method developed in [34] with information obtained from temperature and CO2 sensors, and it is predicted by a queueing model-based approach developed in [35]. The weather conditions including solar radiation and outdoor temperature and humidity are forecasted by the method presented in [36] with the actual data obtained from the meteorological station [32]. By using these methods with the actual data, the range of the prediction error for the case studies in this paper can be estimated. We evaluate the performance of the proposed algorithm over this range in Section 4.4. Furthermore, since any prediction methods can be deployed in the proposed algorithm, we define the relationship between the actual and predicted values of the disturbance in a general way as shown in (24). In this way, prediction results obtained with any method can be described by (24) with a specific $\mathbf{w}^k$. Therefore, we can generate representative scenarios by (24) at different prediction error values of the disturbance, in order to provide a comprehensive quantitative performance analysis of the proposed method with respect to a wide range of the prediction error.

Based on this algorithm, the recalculation of the operational strategy is determined by the triggering of the two events so that recalculation can be avoided at any stage when the thermal comfort is satisfied. The latest strategy is applied until any of the two events is triggered. This process is repeated until the scheduling horizon is covered. Since the computational requirement of the ETM method is not more than that of the time-triggered method if their sampling intervals are the same [26], the proposed ETM-based algorithm can perform well in reducing the communication and computational resources without obvious degradation in the building system performance. Furthermore, building system states and environmental conditions vary moderately, which may provide an advantage when applying the ETM method to the optimization of building operation. The performance of the proposed ETM method is demonstrated using case studies in Section 4.4.

4. Case studies and numerical results

4.1. Accuracy analysis of the approximate PMV model

In this subsection, we evaluate and validate the accuracy of the approximate PMV model developed in this paper. As mentioned earlier, the air velocity, metabolic rate and clothing of occupants are given as prior knowledge and the approximation of the relative humidity can be compensated by the triggering of the events and moving horizon scheme, so we test the performance of the approximate PMV model with respect to the indoor air temperature and mean radiant temperature. In practice, the usual ranges of these two temperatures are both within [15 °C, 35 °C] [23], which is equally divided into 4 segments for the piecewise linearization in both cases. The PMV values obtained with the original PMV model and the approximate PMV model are calculated based on (1)–(6) and (1)–(3), (5), and (18)–(22) over the above-mentioned range respectively. The results are shown in Fig. 2. It is found that the difference between the PMV values obtained by the two models is very small, and the maximal absolute error is less than 0.005, which is negligible from a practical point of view [30]. Generally speaking, the large error occurs in situations when the difference between the indoor air temperature and the mean radiant temperature is larger. But this is an unusual condition in practice. It is also found that when the mean radiant temperature and the indoor air temperature are similar, the error is always less than 0.003. When the mean radiant temperature and the indoor air temperature are both low, the error is about 0.004–0.005. This is because of the approximation of (4).

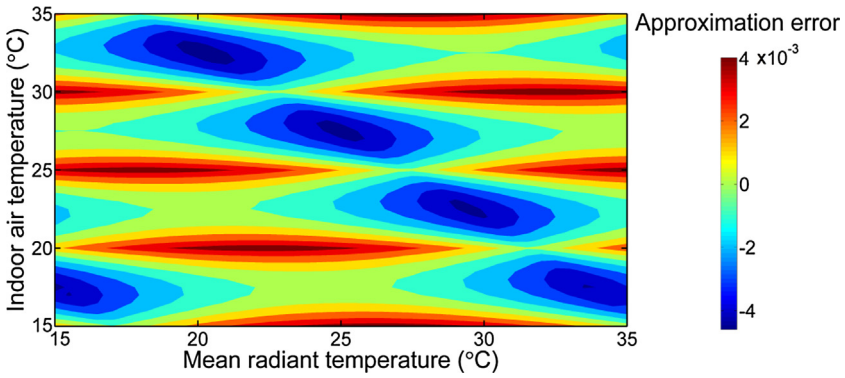

Fig. 2. The error (original PMV-approximate PMV) of the approximation over a temperature range between 15 and 35 °C; air velocity = 0.18 m/s; relative humidity = 55%; metabolic activity = 1.2 met; and clothing insulation = 0.65 clo.

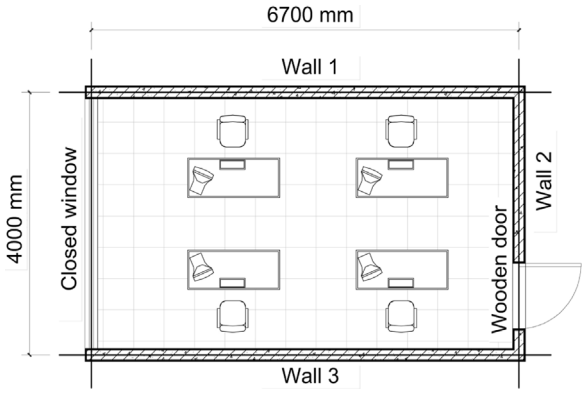

Fig. 3. Structure and configuration of the room.

Since the following case studies are conducted for cooling, the performance of the approximate PMV model is also tested over the usual temperature range of [20 °C, 30 °C] in the mechanically ventilated office environment. In this case, the ranges of the mean radiant temperature and indoor air temperature are also divided into 4 segments. The maximal error of the approximate PMV model is less than 0.002. Therefore, the approximate PMV model is sufficiently accurate for our application and is used to calculate the PMV index in the following case studies with the range partitions mentioned above.

4.2. Set-up of the case studies

In order to minimize the effect of the room model accuracy on the evaluation of the proposed method, we conducted an experiment in an office-room environment in Singapore to produce a room model with high accuracy. As shown in Fig. 3, this room has a closed window and is occupied by four occupants. Its dimensions are 6.7 m × 4 m × 2.85 m. In the room, the indoor air temperature is controlled by the FCU and the indoor humidity is controlled by the DOAS. With the given set-point of the humidity ratio provided by the DOAS, there is little variance in the indoor humidity (about 0.012–0.015 kg/kg) during the whole experiment. This keeps the space at a quasi-constant humidity. So we fix the indoor humidity to 0.014 kg/kg in the calculation of the proposed method. In addition, the floor and roof in this experiment are considered to be isolated from rooms on adjacent floors, since we cannot measure the temperatures of their external surface.

We used a set of two-day (Nov. 11–12 2016) measured data of indoor air temperature, surface temperature of all the walls, cooling supplied by HVAC, solar radiation, and outdoor temperature to identify the optimal parameters of the room model by minimizing the error between the measured temperature and the simulated temperature obtained by the room model based on (8)–(9). The typical values of the parameters in (8)–(9), which are obtained from ASHRAE handbook [31], are used as the initial guesses in this optimization program. This parameter identification problem is solved with the *fmincon* function in MATLAB.

Table 1
Parameter identification of the room model.

Parameter	Value (J/K)	Parameter	Value (m^2 K/W)
C_{wall1}	3.87×10^6	R_w	1.43
C_{wall2}	6.24×10^6	R_{win}	0.13
C_{wall3}	3.63×10^6	R_{in}	0.09
C_a	3.74×10^5	R_{out}	2.91

Note that R_w, R_{win}, R_{in}, and R_{out} are the R-values of wall, window, inside air film and outside air film, respectively.

The optimal parameters are shown in Table 1, and the results of the model identification are shown in Fig. 4(a). With these parameters, we used the measured data (Nov. 13 2016) of the same room to validate the model accuracy. The results of the model validation are shown in Fig. 4(b). It is found that the room model is accurate enough for our application, since a root-mean-square error (RMSE) of only 0.156 is obtained between the measured air temperature and the simulated temperature.

As shown in Fig. 5, we established a mapping from energy consumption to cooling supplied by the HVAC system based on (14), with the measured data in different conditions of the cooling load. If we use a quadratic function to fit the mapping, the cooling supplied decreases with a rise in the energy consumption when the electricity power is less than 0.15 kW. However, it does not work this way in reality. Therefore, as shown in Fig. 5, a cubic polynomial function is used in this paper. For this cubic fit, the R-square value is 0.989 and RMSE is 0.185. Furthermore, in order to make a tradeoff between the model accuracy and amount of computation, a piecewise linear function is developed to approximate this cubic function, which does not introduce much error but significantly reduces the computation time. The maximal relative error of this approximation is less than 4%. Hence, we can compute the simulation results based on the following piecewise linear function instead of (14).

$$\begin{cases} q^k_{fcu} + q^k_{doas} = 1.414 e^k_{hvac}, \ \text{if} e^k_{hvac} \in [0, 0.4], \\ q^k_{fcu} + q^k_{doas} = 3.028 e^k_{hvac} - 0.645, \ \text{if} e^k_{hvac} \in [0.4, 0.6], \\ q^k_{fcu} + q^k_{doas} = 5.283 e^k_{hvac} - 1.998, \ \text{if} e^k_{hvac} \in [0.6, 0.8], \\ q^k_{fcu} + q^k_{doas} = 8.425 e^k_{hvac} - 4.512, \ \text{if} e^k_{hvac} \in [0.8, 1.0], \\ q^k_{fcu} + q^k_{doas} = 12.455 e^k_{hvac} - 8.542, \ \text{if} e^k_{hvac} \in [1.0, 1.2]. \end{cases}$$

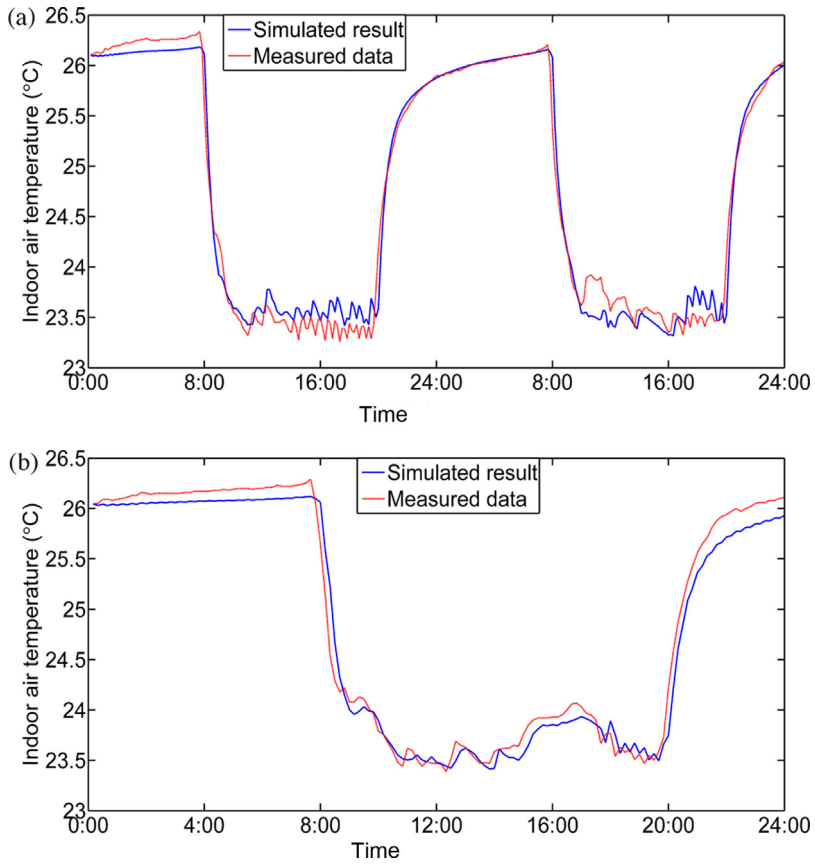

Fig. 4. (a) Identification results of the room model (Nov. 11–12 2016); (b) Validation results of the room model (Nov. 13 2016).

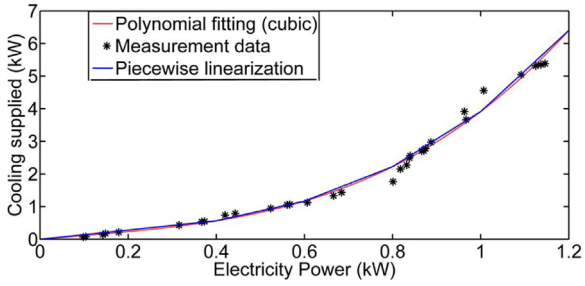

Fig. 5. HVAC model obtained based on the measured data.

4.3. Analysis of energy cost saving and flexibility achieved based on the PMV model

In this subsection, based on the deterministic version of the problem, the performance of predicting the thermal comfort based on the PMV model for building operational optimization is tested. The room and HVAC models shown in Section 4.2 are used in this case. The comfortable range of the PMV index is [−0.5, 0.5], obtained from [23]. For the calculation of the PMV index, the metabolic rate of occupants is set to 1.2 met referring to typical office work, the clothing insulation is set to 0.65 clo according to the calculation shown in [22], and the air velocity is set to 0.18 m/s. The occupancy and the time-of-use (TOU) electricity price are shown in Fig. 6. This test was performed on a hot-humid day (Nov. 15 2016) in Singapore; the weather data are obtained from [32].

The problem with the above data over the scheduling horizon (K = 48, i.e., 24 h are divided into 48 stages) is solved using the CPLEX solver with a relative error gap of 0.01. The calculation is carried out on a Windows PC with a 2.4 GHz CPU and an 8 GB RAM. The results are shown in the second column of Table 2. To analyze the energy cost saving potential based on the PMV model, the problem of describing the thermal comfort with a static range of indoor air temperature (as the usual way) is also solved to obtain a solution for comparison. The results are shown in the third column of Table 2. Note that this given static range of indoor air temperature is [23 °C, 26 °C]. It is obtained from ISO 7730: 2005 [23] corresponding to the comfortable range of the PMV index mentioned above.

Table 2
Comparison on describing the thermal comfort by two ways.

	Proposed solution based on the PMV model	Solution with the given range of temperature
Energy consumption (kWh)	16.6	19.5
Energy cost (S$)	18.8	22.8
Computational time (s)	11	7

In Table 2, it is found that there is not much of a difference in the computational time for these two solutions, which indicates that the approximate PMV model does not significantly increase the computational cost and is thus efficient in the optimization process. The energy consumption and the energy cost of the solution obtained based on the PMV model are less than 14.6% and 19.7% of those obtained with the given range of temperature respectively. These energy and cost savings are achieved by cooling load reduction and load shifting, which are discussed in more detail as follows.

The indoor air temperatures of these two solutions are shown in Fig. 7(a). It is found that the indoor air temperature obtained based on the PMV model is higher than that obtained with the given range of temperature during most of the occupied time. This means that the cooling load of the solution obtained based on the PMV model is lower, and that the energy and cost savings are achieved. It is

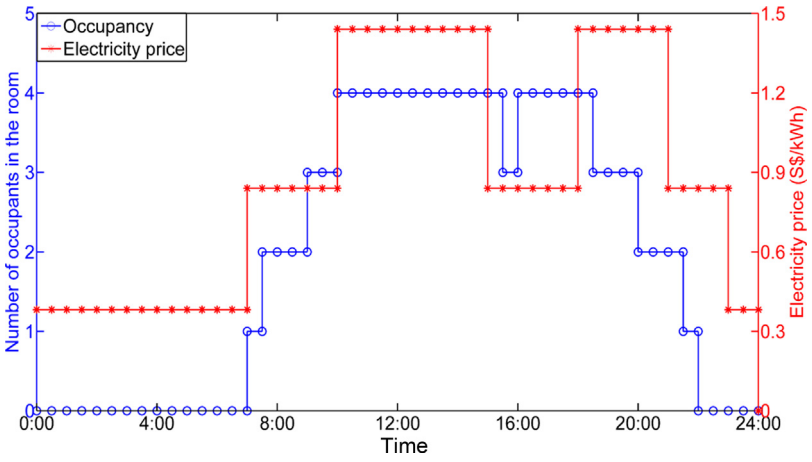

Fig. 6. The occupancy and the TOU electricity price scheme over the scheduling horizon.

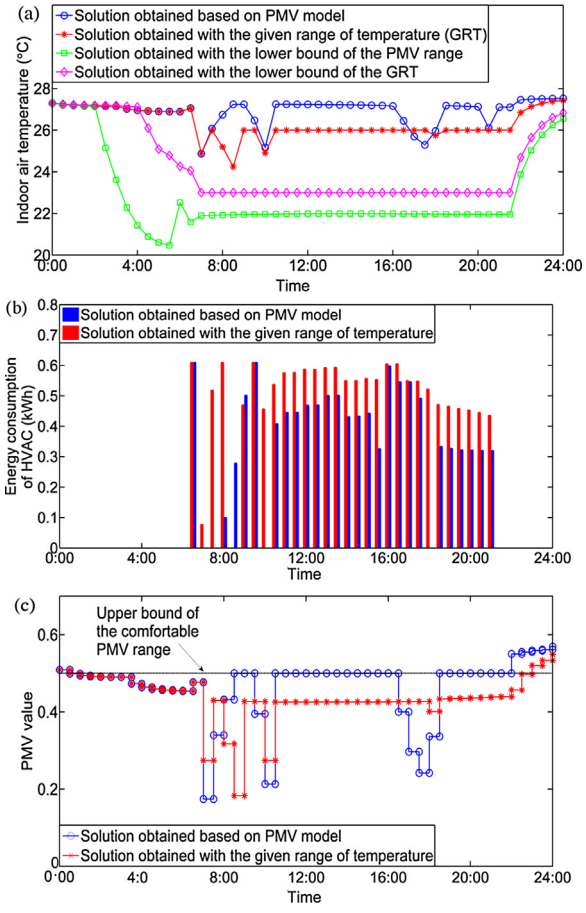

Fig. 7. (a) Comparison of the indoor air temperature; (b) Comparison of the energy consumption of HVAC; (c) Comparison of the PMV values. Note that the energy consumption of the HVAC is the summation of that of the FCU, the DOAS, and other parts of HVAC.

also found in Fig. 7(a) that there are several charging-discharging processes of cooling energy to achieve the load shifting. For example, in the case of the solution obtained based on the PMV model, the indoor air temperature is at a low level to store the cooling energy during 7:00–10:00 and 16:00–18:00, since the electricity price is lower during these periods. The cooling energy stored is then discharged to reduce the energy demand in future peak-price periods such as 10:00–15:00 and 18:00–21:00. In the case of the solution obtained with the given range of temperature, the similar charging-discharging process occurs during 7:30–10:00. The energy consumptions per half hour of the HVAC for these two solutions are shown in Fig. 7(b). The energy consumption of the solution obtained based on the PMV model is lower than that of the solution obtained with the given range of temperature during most of the occupied time due to the cooling load reduction mentioned above. Also, it is found that the difference between these two energy consumptions is bigger during the peak-price periods (such as 10:00–15:00 and 18:00–21:00). This indicates that the solution obtained based on the PMV model responds better to the electricity price signal to give a better reduction in energy cost.

As PMV is a widely accepted index for thermal comfort, we show the PMV values of these two solutions in Fig. 7(c). Note that the PMV value of the solution obtained with the given range of temperature is calculated with values of clothing insulation, metabolic rate and air velocity which are the same as those in the case of using the PMV model. It is found that thermal comfort can be satisfied with both solutions since all PMV values are less than or equal to 0.5 during the occupied time. But in terms of energy consumption and costs, the solution obtained with the given range of temperature is conservative since it is only determined by the indoor air temperature. Therefore, compared to the usual way of describing the thermal comfort by a static range of the air temperature, describing the thermal comfort based on the PMV model can provide more potential on both the energy cost saving for the buildings and the demand reduction for the power grid, since the thermal comfort can be determined by the joint adjustment of the environmental factors through the PMV model and provides more flexibility in response to price signals.

Furthermore, to analyze the flexibility of demand response provided by the PMV model, we solve the problem with the lower bound of the comfortable PMV range (i.e., −0.5) and the lower bound of the given range of temperature (i.e., 23 °C) respectively. The indoor air temperatures of these two solutions are shown in Fig. 7(a). It is found that under the premise of satisfying the thermal requirement, describing the thermal comfort based on the PMV model can provide more availability for demand response as compared to doing so with the given range of temperature, since there are more adjustable range of indoor air temperature (i.e., cooling load) and space for precooling in response to the electricity price signal which can be achieved by using the PMV model. Therefore, the PMV model can not only concretely describe the thermal comfort of occupants, but also provide more flexibility for the optimization of building operation.

Table 3
Performance comparison of the ETM method and MPC method.

	ETM method	MPC method
Mean of the energy costs (S$)	19.54	19.48
Standard deviation (STD) of costs (S$)	0.57	0.58
Mean of the number of recalculations	11.32	48
STD of the number of recalculations	3.48	0

4.4. Performance analysis of the ETM method

In this subsection, the problem described in Section 4.3 is considered under the uncertainties in the outdoor temperature, solar radiation, number of occupants, and occupied time, and it is solved with the ETM method developed in this paper. In order to analyze its performance, we also solve the problem with a typical time-triggered method, i.e., a closed-loop MPC method, to obtain a solution for comparison. The calculation process of the MPC method is: at each stage, the uncertainties are predicted with currently measured data over the next N stages, and the problem is then solved with the measured data and these predictions. Only the strategy at the current stage is applied. This process is repeated until the scheduling horizon is covered [10]. To guarantee fairness, the predictions for the ETM method at any stage when any event is triggered are made the same as those for the MPC method at the same stage. We compare the performance difference of these two methods with a prediction horizon of 48 stages. Then, the impact of the prediction horizon length on the performance of the ETM method is discussed with different combinations of the prediction horizon length and prediction errors. The actual values of the outdoor temperature, solar radiation, number of occupants and occupied time over all stages are assumed to be known in advance, which are the same as those in the case described in Section 4.3. Note that in the following comparisons, the system performance is indicated by the energy costs of the solutions obtained by the ETM and MPC methods, and the computational effort is indicated by the number of recalculations by the two methods over the scheduling horizon.

By applying the prediction methods mentioned in Section 3.2 with the actual data, we found that the prediction error caused by these methods is always less than 20% in our case studies. So, we first evaluate the performance of the ETM method over the range of $\delta \leq 20\%$, where δ is the prediction error and is defined as: $\delta = \lambda / \|\mathbf{d}^k\|_\infty$. We randomly generate 50 scenarios based on (24) with $\delta \leq 20\%$. The solutions obtained with the ETM and MPC methods under these 50 scenarios are applied to the case with the actual values. The results are shown in Table 3. As shown in Table 3, the performance of the ETM method is similar to that of the MPC method, since the mean and standard deviations of the energy costs obtained by the two methods under these 50 scenarios are both similar. However, the mean of the number of recalculations by the ETM method is much less than that by the MPC method. Under these 50 scenarios, the maximal number of recalculations by the ETM method is 16. This means that the ETM method results in a significant reduction in communication and computational resources without perceivable degradation in the system performance as compared to the MPC method. Furthermore, it is also found that the solution obtained by the ETM method is robust with respect to the prediction error, since the standard deviations of the cost and number of recalculations are relatively low.

Second, in order to provide a comprehensive quantitative analysis of the proposed ETM method over a wide range of the prediction error, we assess its performance at different prediction error values of the disturbance. We set δ to 5%, 15%, 20%, 30%, and 50%, and randomly generate predictions by (24) with these prediction errors respectively. For each prediction error, two predictions are randomly generated over all stages. Ten scenarios are thus constructed. The solutions obtained with the ETM method and MPC method under these scenarios are also applied to the case with the actual values, and the results are shown in Fig. 8.

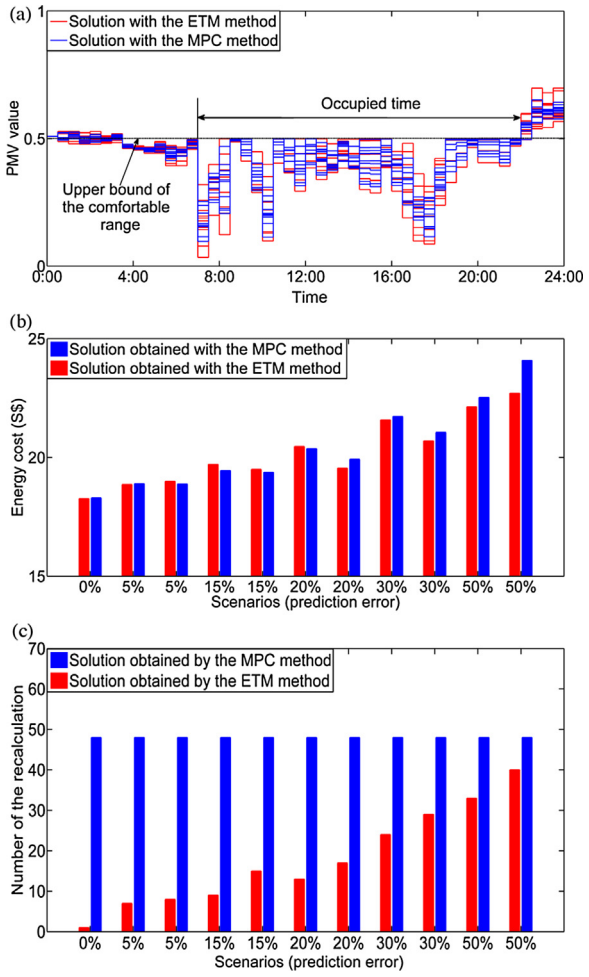

Fig. 8. (a) Comparison of the PMV values; (b) Comparison of the energy cost; (c) Comparison of the computational effort.

It is shown in Fig. 8(a) that the thermal comfort can be satisfied with both methods during the occupied time. The energy costs of these solutions are shown in Fig. 8(b). It is found that in the scenario of no prediction error, the optimal solution is obtained with the ETM method. The energy cost of the solution obtained with the MPC method is slightly higher. This is caused by computation error, since the calculation of the optimal solution should be performed once at each stage with the MPC method. In the scenarios of large prediction errors (such as 30% and 50%), the ETM method outperforms the MPC method since the recalculation of the ETM method is performed when any event is triggered. This may reduce the impact of the imperfect predictions on the system performance. In the scenarios of lower prediction errors (such as 5%–20%), the performance of the ETM method is slightly worse than that of the MPC method in most of these cases, but the degradation is less than 1.9%. Therefore, the two methods have very similar performances with respect to lower prediction errors. The computational efforts by the two methods under these scenarios are also compared. The number of recalculations by the two methods over the scheduling horizon is shown in Fig. 8(c). It is found that the ETM method can significantly reduce the number of recalculations as compared to the MPC method. But along with the increase of prediction error, the number of recalculations increases due to the rise of the number of the events triggered. On average, the ETM method reduces more than

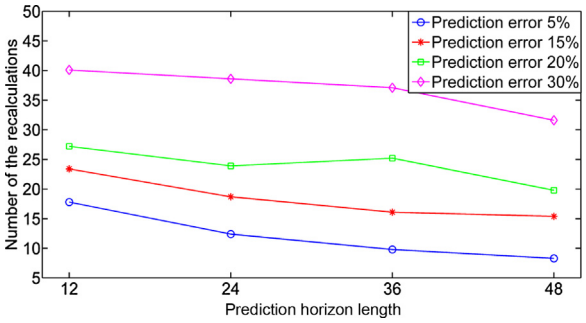

Fig. 9. Computational effort under different combinations of prediction horizon length and prediction error.

60% of the computational effort of the recalculation as compared to the MPC method. It shows that the ETM method can significantly reduce the communication and computational resources for sensor networks and control system in buildings.

Since both the prediction error and horizon length have a significant impact on the computational efficiency of the ETM method, we test the computational effort under different combinations of their values, and show the results in Fig. 9. Note that for each combination, the result is obtained by the average value under 50 scenarios. As shown in Fig. 9, generally speaking, the number of recalculations decreases with the rise of the prediction horizon length but increases with the rise of the prediction error. In the scenarios of higher prediction errors (such as 30%), it is found that the number of recalculations is mainly determined by the prediction error. In the scenarios of lower prediction errors (such as 5%–20%), the variance in the number of recalculations is relatively small in all cases of different prediction horizons. But by choosing the shorter prediction horizon length, the computational time of each recalculation can be significantly reduced. Therefore, we should make a tradeoff between the computational cost of each recalculation and the number of recalculations when deciding the prediction horizon length.

5. Discussion

As mentioned in Section 1, mixed integer programming is widely used to formulate the optimization problem of building operation since the continuous and discrete variables are always involved in practice. In addition, to be efficiently solved, the problem is usually approximately or directly formulated as the mixed integer linear programming problem. So in this paper we also formulate the problem this way. In recent literature, the MPC method has emerged as an effective approach to solve the optimization problem of building operation under uncertainties mainly due to its ability to handle constrained optimal control problems [37] and take the prediction of future system behavior into consideration while satisfying the system constraints [13]. However, MPC method is time-triggered and may thus cause a waste of communication and computational resources due to the recalculation at stages when the building system is operating within a desirable range. This waste may have significant impact on the operation of sensor networks and control system, such as the wireless devices with limited energy. Therefore, we develop a model-based periodic event-triggered mechanism (ETM) method in this paper, in order to reduce the communication and computational resources while providing a solution without perceivable degradation in the system performance as compared to the time-triggered methods. Furthermore, based on the numerical results shown in Section 4.4, it is also found that the ETM method may reduce the impact of large prediction errors on the system performance. In this paper, the ETM method is developed and evaluated in the application of building operational optimization under uncertainties. But it could also be applied to other problems. For example, stochastic dynamic programming (SDP) is a possible choice to formulate the problem under uncertainties, but it may face computational challenges because the state and action spaces increase exponentially with the scale of the problem [15]. So it is an interesting future work to overcome this challenge by integrating the ETM method with SDP approach.

The main focus of this paper is to provide a quantitative performance analysis of the ETM method. In order to minimize the impact of the room model accuracy on the evaluation of the ETM method, we conducted an experiment in an office room in Singapore to produce a room model with high accuracy. Due to the high outdoor temperature and humidity, windows in tropical commercial buildings are almost always closed during the occupied time. Therefore, the room considered in this paper is a representative scenario for the tropical buildings. Although natural ventilation is not considered in this paper, we notice that any extension of the room/building model does not limit the application of the proposed ETM method. For example, if natural ventilation is considered, we just need to replace (9)–(10) by the corresponding equations shown in [25], since our model is derived from the model developed in [25] that can involve the natural ventilation. Moreover, if a room/building is supplied by the multiple energy systems, we just need to add energy balance equations for energy flow from supply to demand and operational constraints for energy generation devices to the model. As shown in many references, such as [9,11,29], the energy balance equation is always linear and the constraints for the energy generation devices are always formulated by the mixed integer linear programming. Therefore, these extensions can easily be integrated with our problem and would not provide any difficulties to the application of the proposed ETM method.

Furthermore, we notice that the proposed ETM method does not limit the problem formulation and the corresponding solution approach. In other words, the ETM method does not depend on the problem modeling. Based on the triggering of predefined events, the ETM method provides an event-triggered manner to decide whether the strategy should be recalculated at each stage. The problem in (25) in step 3 of the proposed algorithm is formulated in a general way to show how the recalculation works by the ETM method. In general, the objective function in (25) can be formulated for different purposes, such as minimizing the energy cost, consumption, or dissatisfaction of thermal comfort. As shown in (25), the constraints include the system dynamic equations, the constraints for input and state variables, and the constraints for thermal requirement, which can also be formulated for any specific applications with different energy devices. For example, if we consider any specific types of the HVAC system for different weather conditions, we just need to modify the operational constraints of the HVAC (i.e., the constraints of input and state variables) in (25) based on the specific types of the HVAC with the corresponding weather conditions. Also, if we consider the problem for multiple rooms, we just need to modify the room model (i.e., the system dynamic equations) in (25) to include the coupling between energy dynamics of the adjacent rooms. These modifications or extensions for specific applications may provide some challenges to the problem modeling and the corresponding solution approach, but they do not provide any difficulties to the application of the ETM method since the implementation of the ETM method is determined by the predefined events that are determined by the system state rather than the problem modeling.

Actually, predefined events play a crucial role in the performance of the ETM method and they should be defined based on specific applications, in order to maximally improve system performance. For example, this paper focuses on a tradeoff between

thermal comfort and energy cost, so we define the two events based on occupancy and thermal comfort index. Based on the numerical results, it is found that these two events are proper since they can provide a huge improvement in computational efficiency as compared to the MPC method. However, these two events may not be suitable for other applications, such as control of the water loop in HVAC system. Therefore, an interesting future work is to study on how to define the proper events for effectively applying the ETM method to different control processes of the building operation. Furthermore, since this paper focuses on the scheduling problem in the upper level of the building control system, another interesting future work is to apply the ETM method to the real-time control in the lower level of the building control system.

6. Conclusions

We proposed and tested a novel building operational optimization approach in which thermal comfort is modeled using the PMV index. We found that describing the thermal comfort based on the PMV model leads to energy and cost savings for the buildings and demand reduction for the power grid. This is due to that it can provide more availability of demand response as compared to doing so using a static range of indoor air temperature. However, directly integrating the PMV model with the optimization of building operation is computationally expensive due to the non-convex and nonlinear properties of the PMV model. We developed an approximation of the PMV model and proved that it is sufficiently accurate and computationally efficient in the optimization of the building operation. We developed and tested a model-based periodic ETM method to efficiently handle the uncertainties in the building operation. The numerical results show that this method is capable of reducing the communication and computational resources, while providing a solution that is robust with respect to the prediction error of the uncertainties.

Acknowledgements

The authors would like to thank the editor and the anonymous reviewers for their valuable comments and suggestions, Dr. Ming Jin and Mr. Evan Putra Limanto from University of California, Berkeley for providing language help and valuable suggestions on the prediction methods, and Dr. Shuo Liu from BEARS for his great help on conducting the experiment.

References

[1] J.H. Yoon, R. Baldick, A. Novoselac, Dynamic demand response controller based on real-time retail price for residential buildings, IEEE Trans. Smart Grid 5 (1) (2014) 121–129.
[2] P.P. Varaiya, F.F. Wu, J.W. Bialek, Smart operation of smart grid: risk-limiting dispatch, Proc. IEEE 99 (1) (2011) 40–57.
[3] U.S. Environmental Protection Agency (EPA), Buildings and Their Impact on the Environment: A Statistical Summary, 2009 http://archive.epa.gov/greenbuilding/web/pdf/gbstats.pdf.
[4] D.B. Crawley, L.K. Lawrie, F.C. Winkelmann, et al., EnergyPlus: creating a new-generation building energy simulation program, Energy Build. 33 (4) (2001) 319–331.
[5] E. Asadi, M.G.D. Silva, C.H. Antunes, L. Dias, A multi-objective optimization model for building retrofit strategies using TRNSYS simulations, GenOpt and MATLAB, Build. Environ. 56 (2012) 370–378.
[6] P.M. Ferreira, A.E. Ruano, S. Silva, E.Z.E. Conceicao, Neural networks based predictive control for thermal comfort and energy savings in public buildings, Energy Build. 55 (2012) (2012) 238–251.
[7] L. Magnier, F. Haghighat, Multiobjective optimization of building design using TRNSYS simulation, genetic algorithm, and artificial neural network, Build. Environ. 45 (2010) 739–746.
[8] Z. Wang, L. Wang, Intelligent control of ventilation system for energy-efficient buildings with CO2 predictive model, IEEE Trans. Smart Grid 4 (2) (2013) 686–693.
[9] A. Anvari-Moghaddam, H. Monsef, A. Rahimi-Kian, Optimal smart home energy management considering energy saving and a comfortable lifestyle, IEEE Trans. Smart Grid 6 (1) (2015) 324–332.
[10] M. Maasoumy, A. Sangiovannin-Vincentelli, Optimal control of building HVAC systems in the presence of imperfect predictions, in: 5th Annual Dynamic Systems and Control Conference, Florida, USA, 2012.
[11] X. Guan, Z. Xu, Q.-S. Jia, Energy-efficient buildings facilitated by microgrid, IEEE Trans. Smart Grid 1 (3) (2010) 243–252.
[12] S. Privara, J. Siroky, L. Ferkl, J. Cigler, Model predictive control of a building heating system: the first experience, Energy Build. 43 (2011) (2011) 564–572.
[13] R. Kwadzogah, M. Zhou, S. Li, Model predictive control for HVAC systems –a review, in: IEEE International Conference on Automation Science and Engineering, Madison, USA, 2013.
[14] B. Sun, P.B. Luh, Q.-S. Jia, B. Yan, Event-based optimization within the Lagrangian relaxation framework for energy savings in HVAC systems, IEEE Trans. Autom. Sci. Eng. 12 (4) (2015) 1396–1406.
[15] Z. Wu, Q.-S. Jia, X. Guan, Optimal control of multiroom HVAC system: an event-based approach, IEEE Trans. Control Syst. Technol. 24 (2) (2016) 662–669.
[16] S. Yordanova, D. Merazchiev, L. Jain, A two-variable fuzzy control design with application to an air-conditioning system, IEEE Trans. Fuzzy Syst. 23 (2) (2015) 474–481.
[17] H. Zhang, A. Davigny, F. Colas, Y. Poste, B. Robyns, Fuzzy logic based energy management strategy for commercial buildings integrating photovoltaic and storage systems, Energy Build. 54 (2012) (2012) 196–206.
[18] M. Hamdy, A. Hasan, K. Siren, Impact of adaptive thermal comfort criteria on building energy use and cooling equipment size using a multi-objective optimization scheme, Energy Build. 43 (2011) (2011) 2055–2067.
[19] M. Frontczak, S. Schiavon, J. Goins, E. Arens, H. Zhang, P. Wargocki, Quantitative relationships between occupant satisfaction and satisfaction aspects of indoor environmental quality and building design, Indoor Air 22 (2) (2012) 119–131.
[20] P. Fanger, Thermal Comfort: Analysis and Applications in Environmental Engineering, Danish Technical Press, Copenhagen, 1970.
[21] J. Cigler, S. Privara, Z. Vana, D. Komarkova, M. Sebek, Optimization of predicted mean vote thermal comfort index within model predictive control framework, in: 51st IEEE Conference on Decision and Control, Hawaii, USA, 2012.
[22] ASHRAE Standard 55-2013, Thermal Environmental Conditions for Human Occupancy, ASHRAE Handbook Fundamentals, American Society of Heating Refrigerating and Air Conditioning Engineers, Inc., 2013.
[23] ISO7730, 2005, Ergonomics of the Thermal Environment-Analytical Determination and Interpretation of Thermal Comfort Using Calculation of PMV and PPD Indices and Local Thermal Comfort Criteria, International Organization for Standardization, 2005.
[24] M. Maasoumy, A. Pinto, A. Sangiovanni-Vincentelli, Model-based hierarchical optimal control design for HVAC systems, in: Proceedings of the ASME 2011 Dynamics System and Control Conference (DSCC 2011), Arlington, VA, USA, 2011.
[25] B. Sun, P.B. Luh, Q.S. Jia, Z. Jiang, F. Wang, C. Song, Building energy management: integrated control of active and passive heating, cooling, lighting, shading, and ventilation systems, IEEE Trans. Autom. Sci. Eng. 10 (3) (2013) 588–602.
[26] W.P.M.H. Heemels, M.C.F. Donkers, Model-based periodic event-triggered control for linear systems, Automatica 49 (2013) (2013) 698–711.
[27] X.R. Cao, J. Zhang, Event-based optimization of markov systems, IEEE Trans. Autom. Control 53 (4) (2008) 1076–1082.
[28] Q.-S. Jia, On solving optimal policies for finite-stage event-based optimization, IEEE Trans. Autom. Control 56 (9) (2011) 2195–2200.
[29] Z. Xu, Q.-S. Jia, X. Guan, X. Xie, A new method to solve large-scale building energy management for energy saving, IEEE International Conference on Automation Science and Engineering (CASE) (2014) 940–945.
[30] F.R. d'A. Alfano, B.L. Palella, G. Riccio, The role of measurement accuracy on the thermal environment assessment by means of PMV index, Build. Environ. 46 (7) (2011) 1361–1369.
[31] Handbook ASHRAE Fundamentals American Society of Heating Refrigerating and Air Conditioning Engineers, 2001.
[32] http://www.weather.gov.sg/.
[33] Z. Xu, S. Liu, G. Hu, C.J. Spanos, Optimal coordination of air conditioning system and personal fans for building energy efficiency improvement, Energy Build. 141 (2017) (2017) 308–320.
[34] M. Jin, N. Bekiaris-Liberis, K. Weekly, C.J. Spanos, A.M. Bayen, Occupancy detection via environmental sensing, IEEE Trans. Autom. Sci. Eng. (2016), http://dx.doi.org/10.1109/tase.2016.2619720.
[35] R. Jia, C.J. Spanos, Occupancy modelling in shared spaces of buildings: a queueing approach, J. Build. Perform. Simul. 10 (4) (2017) 406–421.
[36] O. Erdinç, A. Taşcıkaraoğlu, N.G. Paterakis, Y. Eren, J.P.S. Catalão, End-user comfort oriented day-ahead planning for responsive residential HVAC demand aggregation considering weather forecasts, IEEE Trans. Smart Grid 8 (1) (2017) 362–372.
[37] S. Privara, Z. Váňa, E. Žáčeková, J. Cigler, Building modeling: selection of the most appropriate model for predictive control, Energy Build. 55 (2012) (2012) 341–350.